Journal of Dentistry 130 (2023) 104426

Contents lists available at ScienceDirect

Journal of Dentistry

journal homepage: www.elsevier.com/locate/jdent

Influence of alveolar ridge morphology and guide-hole design on the accuracy of static Computer-Assisted Implant Surgery with two implant macro-designs: An *in vitro* study

Fabrice Alain Dulla [a], Emilio Couso-Queiruga [b], Vivianne Chappuis [c], Burak Yilmaz [d,e,f], Samir Abou-Ayash [g], Clemens Raabe [h,*]

[a] *Department of Oral Surgery and Stomatology; School of Dental Medicine, University of Bern, Switzerland*
[b] *ITI Scholar, Department of Oral Surgery and Stomatology; School of Dental Medicine, University of Bern, Switzerland*
[c] *Chair, Department of Oral Surgery and Stomatology; School of Dental Medicine, University of Bern, Switzerland*
[d] *Faculty member, Department of Reconstructive Dentistry and Gerodontology; School of Dental Medicine, University of Bern, Switzerland*
[e] *Department of Restorative, Preventive and Pediatric Dentistry, School of Dental Medicine, University of Bern, Bern, Switzerland*
[f] *Division of Restorative and Prosthetic Dentistry, The Ohio State University College of Dentistry, Columbus, OH, USA*
[g] *Deputy Department Chair, Department of Reconstructive Dentistry and Gerodontology; School of Dental Medicine, University of Bern, Switzerland*
[h] *Senior Lecturer, Department of Oral Surgery and Stomatology; School of Dental Medicine, University of Bern, Switzerland*

A R T I C L E I N F O

Keywords:
Dental implant
Single tooth
Digital imaging/radiology
Image-guided surgery
Static computer assisted implant surgery
Surgical guide

A B S T R A C T

Objectives: The primary aim of this *in vitro* study was to evaluate the influence of alveolar ridge morphologies on the accuracy of static Computer-Assisted Implant Surgery (sCAIS). The secondary aims were to evaluate the influence of guide-hole design and implant macro-design on the accuracy of the final implant position.

Methods: Eighteen standardized partially edentulous maxillary models with two different types of alveolar ridge morphologies were used. Each model was scanned via cone beam computer tomography prior to implant placement and scanned with a laboratory scanner prior to and following implant placement using sCAIS. The postsurgical scans were superimposed on the initial treatment planning position to measure the deviations between planned and postsurgical implant positions.

Results: Seventy-two implants were equally distributed to the study groups. Implants placed in healed alveolar ridges showed significantly lower mean deviations at the crest (0.36 ± 0.17 mm), apex (0.69 ± 0.36 mm), and angular deviation (1.86 ± 0.99°), compared to implants placed in fresh extraction sites (0.80 ± 0.29 mm, 1.61 ± 0.59 mm, and 4.33 ± 1.87°; all $p<0.0001$). Implants placed with a sleeveless guide-hole design demonstrated significantly lower apical (1.02 ± 0.66 mm) and angular (2.72 ± 1.93°) deviations compared to those placed with manufacturer's sleeves (1.27 ± 0.67 mm; $p = 0.01$, and 3.46 ± 1.9°; $p = 0.02$). Deep-threaded tapered bone level implants exhibited significantly lower deviations at the crest (0.49 ± 0.28 mm), apex (0.97 ± 0.63 mm), and angular deviations (2.63 ± 1.85°) compared to shallow-threaded parallel-walled bone level implants (0.67 ± 0.34 mm; $p = 0.0005$, 1.32 ± 0.67 mm; $p = 0.003$, and 3.56 ± 1.93°; $p = 0.01$).

Conclusions: The accuracy of the final implant position with sCAIS is determined by the morphology of the alveolar ridge, the design of the guide holes, and the macrodesign of the implant.

Clinical Significance: Higher accuracy in the final implant position was observed with implants placed in healed alveolar ridge morphologies, in implants with deep-threaded tapered macro-design, and when sleeveless surgical guide holes were used.

1. Introduction

The correct 3D implant position is crucial for successful treatment outcomes in tooth replacement therapy via dental implants. Planning the ideal 3D implant position involves both prosthetic and anatomical considerations. However, achieving the preoperatively planned 3D implant position might be challenging when using freehanded implant placement protocols [1]. To support the clinician achieve ideal implant

* Corresponding author.
E-mail address: clemens.raabe@unibe.ch (C. Raabe).

https://doi.org/10.1016/j.jdent.2023.104426
Received 18 November 2022; Received in revised form 5 January 2023; Accepted 14 January 2023
Available online 15 January 2023

positioning, computer-aided implant placement protocols have become common in daily clinical practice as digital knowledge and computer-aided manufacturing technologies have advanced [2–4]. Among them, static Computer-Assisted Implant Surgery (sCAIS) has shown high clinical effectiveness and accuracy as compared to other treatment modalities [5–10].

The fabrication of sCAIS guides is based on a digital workflow using standardized tessellation language (STL) and Digital Imaging and Communication in Medicine (DICOM) files. Utilizing this digital workflow has potential to introduce several errors which may contribute to reducing the precision and accuracy of the final implant position. Some of these critical errors have been related to the imaging process, data transfer and matching in the digital planning software, the surgical guide fabrication process, inaccurate guide position and support, free drilling distance, guide-hole design and drill errors [9,11–17]. Improvements in image quality in CBCTs and scanning technology, the introduction of artificial intelligence in planning software, and improved precision of 3D printers have continuously reduced these sources of errors related to the manufacturing process on sCAIS procedures [18].

While the accuracy of sCAIS procedures has been shown to be affected by fabrication-related errors, several other factors which may influence the final implant position have not been fully investigated yet. These potential sources of error are related to therapeutic procedures, surgical interventions, and implant-specific characteristics. One factor might be the timing of implant placement after tooth extraction, correlating with the remodeling of the alveolar ridge's morphology over time [19,20]. Dental implant placement can be carried out immediately (type I, fresh extraction socket), 4–8 weeks (type II, early soft tissue healing), 3–4 months (type III, partial bone healing), or more than 4 months after tooth extraction (type IV, full bone healing) depending on local, systemic, surgical, and prosthetic factors [21,22]. The presence of various ridge morphologies may affect the trajectory of surgical drills and dental implants during the sCAIS procedure and result in deviations from pre-operative planning [9]. The second factor is the feasibility of implant placement utilizing sCAIS without manufacturer's sleeves (i.e., sleeveless). Sleeveless guide holes reduce overall instrument tolerance, total cost, manufacturing time and require less space [15,23,24]. Nonetheless, this type of guide-hole design is technique-sensitive and must be carefully controlled by the implant surgeon (i.e., correct dimensions of the guide-hole, adequate hole offset, and the use of a precise 3D printer) to obtain similar or lower 3D deviations than obtained with manufacturer's sleeve. Interestingly, as an additional factor of error, recent *in vitro* and clinical studies have reported on inter-manufacturer and inter-system differences when evaluating the accuracy of final implant positions, where tolerances of surgical components and implant macro-design may play a crucial role [13,25,26].

There is limited knowledge of the potential sources of errors related to local anatomical characteristics, surgical protocols, and implant-specific characteristics. In order to broaden the knowledge of the effect of the abovementioned factors on the accuracy and predictability of sCAIS procedures, this *in vitro* study primarily aimed to evaluate the influence of alveolar ridge morphology on the accuracy of implant placement. The secondary aims were to evaluate the influence of guide-hole design and implant macro-design implant features on the accuracy of the final implant position. The 0-hypotheses were that the alveolar ridge morphology ($H0_1$), guide-hole design ($H0_2$) and the implant macro-design ($H0_3$) would not influence the positional accuracy of sCAIS implant procedures.

2. Materials and methods

2.1. Study design and setting

This *in vitro* study was conducted in the Department of Oral Surgery and Stomatology at the University of Bern, Switzerland between November 2021 to February 2022.

2.2. Model selection and preparation

Standardized partially edentulous maxillary models simulating natural bone density D2 [27] without soft tissue parts (BoneModels, Castellón de la Plana, Spain) were used in this study. Each model had six single-tooth edentulous sites with either a clinical scenario simulating a healed ridge (FDI positions 16, 14 and 25) or a fresh extraction socket (12, 21 and 23) as shown in Fig. 1A.

Before implant placement, each study model was scanned using a laboratory scanner (3Shape 4, 3Shape Inc, Copenhagen, Denmark) and a cone beam computed tomographic (CBCT) scan (8 × 5 cm, 80μm voxel size, 90kVp, 1mAs; 3D Accuitomo 170, J. Morita Corp, Osaka, Japan) of each model was obtained. The resulting STL and DICOM files were imported to an implant planning software (coDiagnostiX, version 10.5, Dental Wings Inc, Montreal, Canada). One experienced clinician (C.R) planned an ideal 3D implant position considering the anatomical characteristics of the site and prosthetic parameters based on a digital wax-up made by a dental technician (Zirkonzahn.Modellier, Zirkonzahn GmbH, Gais, Italy). Each implant position was digitally planned to support a screw-retained single implant crown.

2.3. Implant system and guide design

The study involved two different implant macro-designs and two guide-hole designs.

The guide-hole designs were as follows (Fig. 1A and B):

- Standard manufacturer's sleeve (MS) (stainless-steel sleeve, and polyether-ether-ketone sleeve).
- Sleeveless sites (SL), where the dimensions of the manufacturer's sleeve were incorporated into the surgical guide.

The dental implants utilized in this study were as follows (Fig. 1C):

- Parallel-walled and self-tapping bone-level implants with a shallow thread depth and a thread pitch of 0.8 mm (BL 4.1 × 12 mm RC, Straumann AG. Basel, Switzerland).
- Tapered and self-tapping bone-level implants with a deep-thread depth and a thread pitch of 2.25 mm (BLX 4.0 × 12 mm RB, Straumann AG. Basel, Switzerland).

2.4. Surgical guide preparation and standardization

Guide-hole calibration matrices with various offsets were tested independently by three investigators with experience in sCAIS (C.R, F.A. D, S.A.A) to define the offset with the best handling and fit of surgical instruments (BL MS: + 0.02 mm, BL SL: + 0.02 mm, BLX MS: + 0.02 mm, BLX SL: + 0.09 mm). In each model, the groups were randomly assigned to obtain an equally distributed sample size. Further variables, including the distance from the implant platform to the sleeve (6 mm), the free drilling distance (18 mm), and the height of instrument guidance (6 mm), were standardized for all groups. The guide material thickness was set to 3.5 mm and the guide-to-teeth offset to 0.15 mm. Multiple fenestrations were created to allow visualization of the guide's intra-operative fit on the model. All guides were manufactured using the identical transparent, light-cured resin for stereolithography (ProArt Print Splint, Ivoclar Vivadent AG, Schaan, Lichtenstein) in a 3D printer (PrograPrint PR5, Ivoclar Vivadent AG, Schaan, Lichtenstein) by the same dental technician and stored in a dark room for maximum of one week upon usage.

2.5. Implant placement procedure on the model

For implant placement, the models were mounted in a phantom

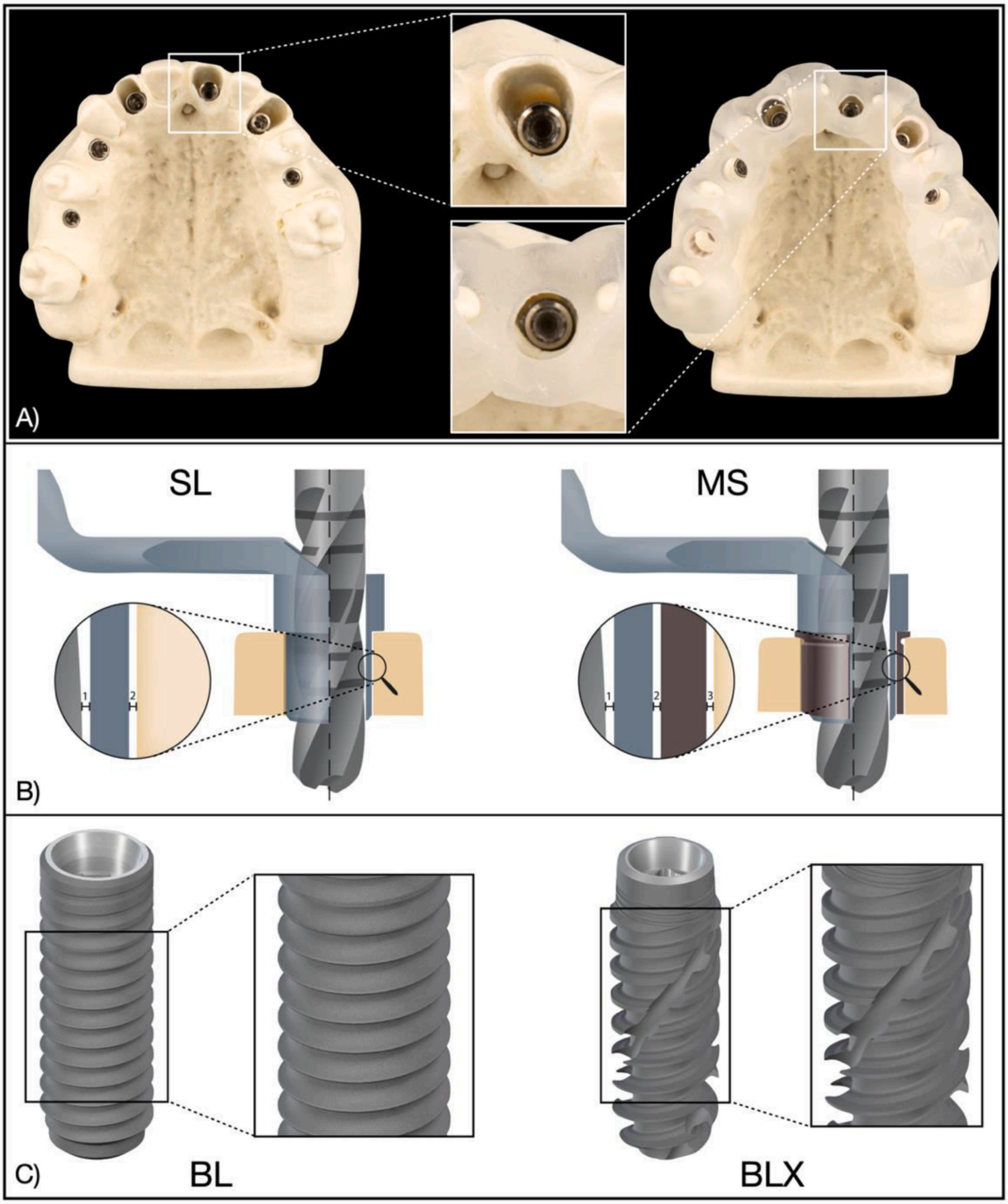

Fig. 1. Representative case of a model with different alveolar ridge morphologies, such as fresh extraction sockets and healed ridges (A), with a surgical guide with different guide-hole designs (A, and B). Sleeveless sites (SL) include two gaps: (1) drill – key; (2) key – guide (manufacturer's sleeve dimensions are incorporated into the guide itself). Standard manufacturer's sleeve (MS) includes three gaps: (1) drill – key; (2) key – MS; (3) MS – guide. Different implant macro-design (C). BL: Parallel-walled with a shallow thread depth bone level implant; BLX: Tapered with a deep thread depth bone level implant. "© Institut Straumann AG, 2022. All rights reserved. By courtesy of Institut Straumann AG.".

head. One experienced and board-certified oral surgeon (C.R) performed all implant placement procedures via sCAIS according to the manufacturer's recommendations using a surgical motor (iChiropro, Bien Air, Bienne, Switzerland).

2.6. Data acquisition and digital measurements

Once the implants were placed, corresponding scan bodies were inserted into the implants following the manufacturer's recommendations. After hand-tightening, including mechanical testing (i.e. until tactile resistance was encountered), direct visual verification of the scan bodies seating was performed. A post-operative scan of each model was made utilizing the same laboratory scanner (3Shape 4, 3Shape Inc, Copenhagen, Denmark) to obtain postoperative STL files. The postoperative STL files were imported to the treatment evaluation tool of the implant planning software (coDiagnostiX, version 10.5, Dental Wings Inc, Montreal, Canada). A corresponding virtual implant and scanbody were superimposed in the postoperative STL-file using a local best-fit algorithm, which works on the basis of a point cloud with 150 reference points placed at the top of the scanbody. Subsequently, the linear and angular deviations between planned and final implant positions were automatically measured by the software's algorithm for the mid-central points of the implant shoulder and implant apex, as shown in Fig. 2.

2.7. Statistical analysis

After the preparation of six models, a power analysis was conducted to find the required minimum number of implant sites to detect significant differences between factors morphology of the alveolar ridge (fully healed ridge, fresh extraction socket), guide-hole design (MS, SL), and implant macro-design (BL, BLX) in at least 80% of all cases; the analysis indicated the need for a total of 18 models. Using a three-way non-parametric ART-ANOVA, all three factors were simultaneously evaluated [28]. All collected data was descriptively summarized by using mean/sd/min/Q1/median/Q3/max statistics showing box plots and tables. A non-parametric three-way ANOVA was conducted for each factor "morphology of the alveolar ridge" (healed, socket), "guide-hole design" (MS, SL), and "implant macro-design" (BL, BLX) including up to two-way interactions [28]. The p-values < 0.05 were considered statistically significant. All statistical analyses were performed with the software R, version 4.0.4 [29] to evaluate the study groups: healed ridge, fresh extraction socket, MS, SL, BL, and BLX.

3. Results

3.1. Characteristics of included specimens

In the total of 18 models, clinical scenarios were simulating $n = 36$ fresh extraction sockets and $n = 36$ healed ridges. In these clinical scenarios, $n = 36$ BL and $n = 36$ BLX implants were placed using sCAIS with an MS ($n = 36$) or SL ($n = 36$) guide-hole design. A total of 18 different surgical guides changing the guide-hole design position to make an equally distributed sample was utilized in this study.

3.2. Deviation outcomes according to different variables

All linear and angular deviation measurements according to different variables are shown in Table 1. Statistically significant angular, crestal, and apical deviations ($p<0.0001$) were observed when the morphology of the alveolar ridge was evaluated. Similarly, statistically significant angular ($p = 0.01$), crestal ($p = 0.0005$) and apical ($p = 0.003$) deviations were observed when the implant macro-design was investigated. The guide-hole design showed statistically different angular deviations ($p = 0.02$), apical deviations ($p = 0.003$), and almost resulted in a statistically significant difference at the crestal level ($p = 0.06$). The interaction term analysis combining variables (i.e., the alveolar ridge morphology: implant macro-design, the alveolar ridge morphology: guide-hole design, implant macro-design: guide-hole design) did not show any statistically significant differences (Table 2).

3.3. Alveolar ridge morphology

A statistically significant lower deviation was observed in implants placed at clinical scenarios simulating fully healed alveolar ridges than in clinical scenarios simulating immediate implant placements in fresh extraction sockets. Implants placed in fully healed alveolar ridges showed mean deviations at the crest of 0.36 ± 0.17 mm, apex 0.69 ± 0.36 mm, and angular deviation of 1.86 ± 0.99° and implants in fresh extraction sockets 0.80 ± 0.29 mm, 1.61 ± 0.59 mm, and 4.33 ± 1.87°, respectively as shown in Table 1 and Fig. 3. In all cases, it was observed both clinically and digitally that the trajectory of deviation in fresh extraction sockets was directed to the alveolus (path of less resistance), whilst for healed sites, deviations from initial planning were found in all directions, as shown in Fig. 4.

3.4. Guide-hole design

Implants placed using the manufacturer's sleeve showed statistically higher mean apical (1.27 ± 0.67 mm) and angular (3.46 ± 1.9°) deviations compared with sleeveless sites (1.02 ± 0.66 mm, and 2.72 ± 1.93°, respectively). A trend for higher deviations at the crestal aspect was observed without statistically significant differences between surgical guides with manufacturer's sleeve vs sleeveless sites (0.63 ± 0.30 mm vs 0.54 ± 0.34 mm, respectively), as observed in Table 1 and Fig. 3.

3.5. Implant macro-design

Statistically significantly lower deviations were observed when BLX implants were placed compared to BL implants, as shown in Table 1 and Fig. 3. BLX implants showed a mean deviation of 0.49 ± 0.28 mm at the crest, 0.97 ± 0.63 mm at the apex, and a mean angular deviation of 2.63 ± 1.85° BL implants mean deviations were 0.67 ± 0.34 mm at the crest, 1.32 ± 0.67 mm at the apex, and a mean angular deviation of 3.56 ±

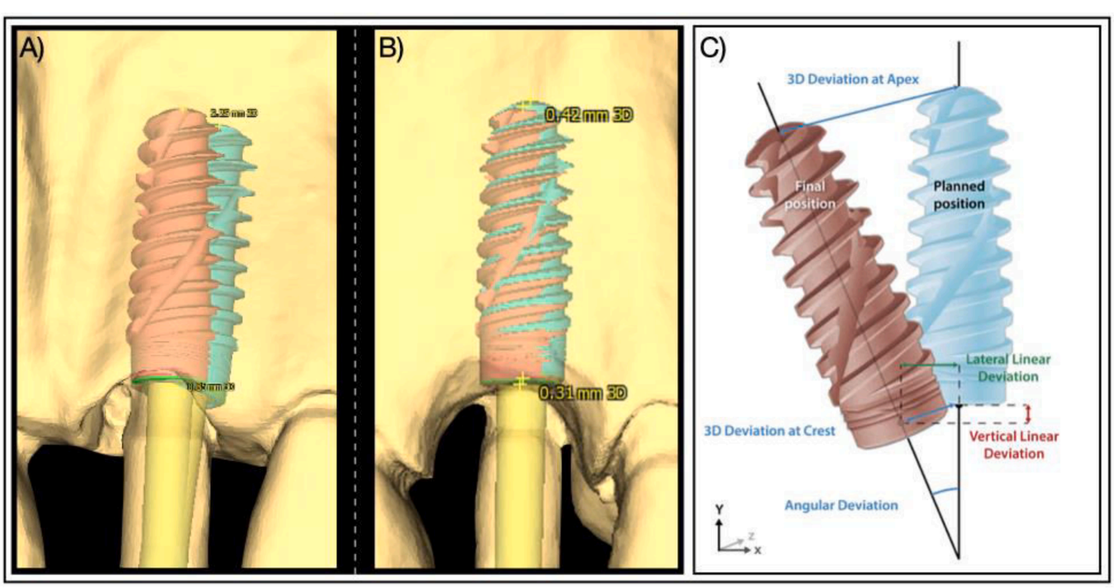

Fig. 2. Deviation between preoperatively planned (blue) and final postoperative implant position (red). Representative example of an implant in an extraction socket (A) and healed alveolar ridge (B). Crestal, apical, and angular 3D deviation (C).

Table 1
Descriptive statistics of angular, crestal, and apical 3D implant deviation for the evaluation of the alveolar ridge morphology, implant macro-design, and guide-hole design. BL: Parallel-walled bone-level implant. BLX: Tapered bone-level implant. MS: Manufacturer's guide-hole design. SL: Sleeveless guide-hole design. NS: not significant / S: significant for all measurement categories.

		N	Mean	SD	Min	Q1	Median	Q3	Max
3D deviation crest (mm)									
Alveolar ridge morphology. S	healed ridge	36	**0.36**	0.17	0.06	0.26	**0.33**	0.42	0.99
	extraction socket	36	**0.80**	0.29	0.24	0.61	**0.83**	0.91	1.51
Implant macro-design. S	BL	36	**0.67**	0.34	0.18	0.37	**0.6**	0.9	1.51
	BLX	36	**0.49**	0.28	0.06	0.27	**0.35**	0.68	1.12
Guide-hole design. NS	MS	36	**0.63**	0.30	0.19	0.33	**0.58**	0.85	1.31
	SL	36	**0.54**	0.34	0.06	0.27	**0.43**	0.75	1.51
3D deviation apex (mm)									
Alveolar ridge morphology. S	healed ridge	36	**0.69**	0.36	0.24	0.48	**0.56**	0.80	2.18
	extraction socket	36	**1.61**	0.59	0.41	1.18	**1.68**	1.98	2.75
Implant macro-design. S	BL	36	**1.32**	0.67	0.38	0.60	**1.27**	1.80	2.75
	BLX	36	**0.97**	0.63	0.24	0.5	**0.75**	1.51	2.31
Guide-hole design. S	MS	36	**1.27**	0.67	0.24	0.60	**1.17**	1.83	2.61
	SL	36	**1.02**	0.66	0.29	0.50	**0.72**	1.53	2.75
Angular deviation (°)									
Alveolar ridge morphology. S	healed ridge	36	**1.86**	0.99	0.3	1.2	**1.6**	2.3	5.8
	extraction socket	36	**4.33**	1.87	0.5	3.37	**4.5**	5.725	8
Implant macro-design. S	BL	36	**3.56**	1.93	1	1.65	**3.35**	4.7	8
	BLX	36	**2.63**	1.85	0.3	1.35	**2**	3.7	6.8
Guide-hole design. S	MS	36	**3.46**	1.9	0.8	2	**3**	5.22	7.1
	SL	36	**2.72**	1.93	0.3	1.2	**2**	3.87	8

Table 2
ANOVA results showing the *p*-values of the alveolar ridge morphology, implant macro-design and guide-hole design, and their combination, with *p*-values <0.05 displayed underlined.

	Angular deviation	3D deviation crest	3D deviation apex
Alveolar ridge morphology	≤0.0001	≤0.0001	≤0.0001
Implant macro-design	0.01	0.0005	0.003
Guide-hole design	0.02	0.06	0.01
Alveolar ridge morphology: Implant macro-design	0.26	0.38	0.37
Alveolar ridge morphology: Guide-hole design	0.83	0.92	0.94
Implant macro-design: Guide-hole design	0.74	0.69	0.71

1.93° was calculated.

4. Discussion

The present investigation examined potential sources of errors related to local anatomical characteristics, surgical protocols, and implant-specific characteristics on the accuracy of implant placement via sCAIS. The results demonstrated higher accuracy in the final implant position in healed alveolar ridges compared to extraction sockets, leading to a facial drift of the implant position, with sleeveless compared to manufacturer's sleeve guide-hole design, and BLX compared to BL implants. Therefore $H0_1$, $H0_2$, and $H0_3$ were rejected.

Alveolar ridge morphology significantly influenced the accuracy of sCAIS. Implants placed in fresh extraction sockets showed statistically significantly higher 3D crestal, apical, and angular deviations than implants placed in healed alveolar ridges. These findings are in accordance with previous publications, where higher 3D deviation was observed in implants placed in fresh extraction sockets as compared to fully healed ridges [9,12,30]. Interestingly, in all implants placed at fresh extraction sockets, the implant position deviated to the zone of less resistance (i.e., the alveolar socket). One possible hypothesis, as described by Wang and coworkers, might be the deflection of the drill by the bony socket walls causing a shift into the socket in a more facial implant placement [30]. This result of a potential facial shift of implant preparation and/or insertion using sCAIS in extraction sockets is of major interest during the preoperative planning and the surgical execution to avoid facial implant malpositioning.

On the other hand, the results highlight the importance for the implant surgeon to critically evaluate the clinical orientation of the implant position throughout the surgery to detect potential 3D malposition and correct it in a freehanded manner, if necessary. Although it was not evaluated in this study, the authors believed that this information could be extrapolated to cases of early implant placement [22] when only soft tissue healing after tooth extraction has taken place. Considering the deviations in the upper quartile of the present study of 1.98 mm, it seems advisable to plan a safety distance of at least 2 mm to critical anatomic structures in the apex area when immediate or early implant placement is planned.

With respect to the guide-hole design, the SL group showed statistically significantly less deviation at the apex and angular deviation as compared with the MS group. Additionally, the SL group showed a trend for less deviation without statistical significance in the crestal aspect. Similar patterns observed in this study were also in agreement with a recent systematic review [31] and with previous preclinical studies [11, 32]. The results observed in this study could be explained by the reduction of the tolerance between the components of the surgical guide. MS surgical guides have three gaps (guide-MS, MS-key, and key-drill), while SL surgical guides have only two gaps (guide-key, and key-drill). Each gap is adding tolerances for the guide, sleeve, and surgical instruments. Therefore, SL guides additionally offer the benefit to modify the tolerance of the gap "guide-key" using varying guide-hole offsets. Small guide hole offsets will result in a more precise fit of the key in the guide hole [33]. In turn, a very precise fit hampers the mounting and dismounting of the key and guide, thereby affecting the handling of the surgical instruments. Furthermore, all-resin SL guides facilitate precise guidance in cases of narrow single-tooth gaps (i.e., maxillary lateral incisors) as the potentially conflicting outer diameter of the MS is not of interest for SL guide-hole design. Lastly, SL guides allow overall cost reduction in the fabrication process, as no charges apply for MS. For the correct interpretation of the results, it must be noted that the offset in the SL group was defined in the software only after the printer matrix had been calibrated by three experienced sCAIS operators. Such calibration is recommended for each lab set-up, as the accuracy of the guide manufacturing process depends on various factors such as the 3D printer used, the material [34], or the printing orientation [35]. Besides varying accuracies obtained using sCAIS systems of

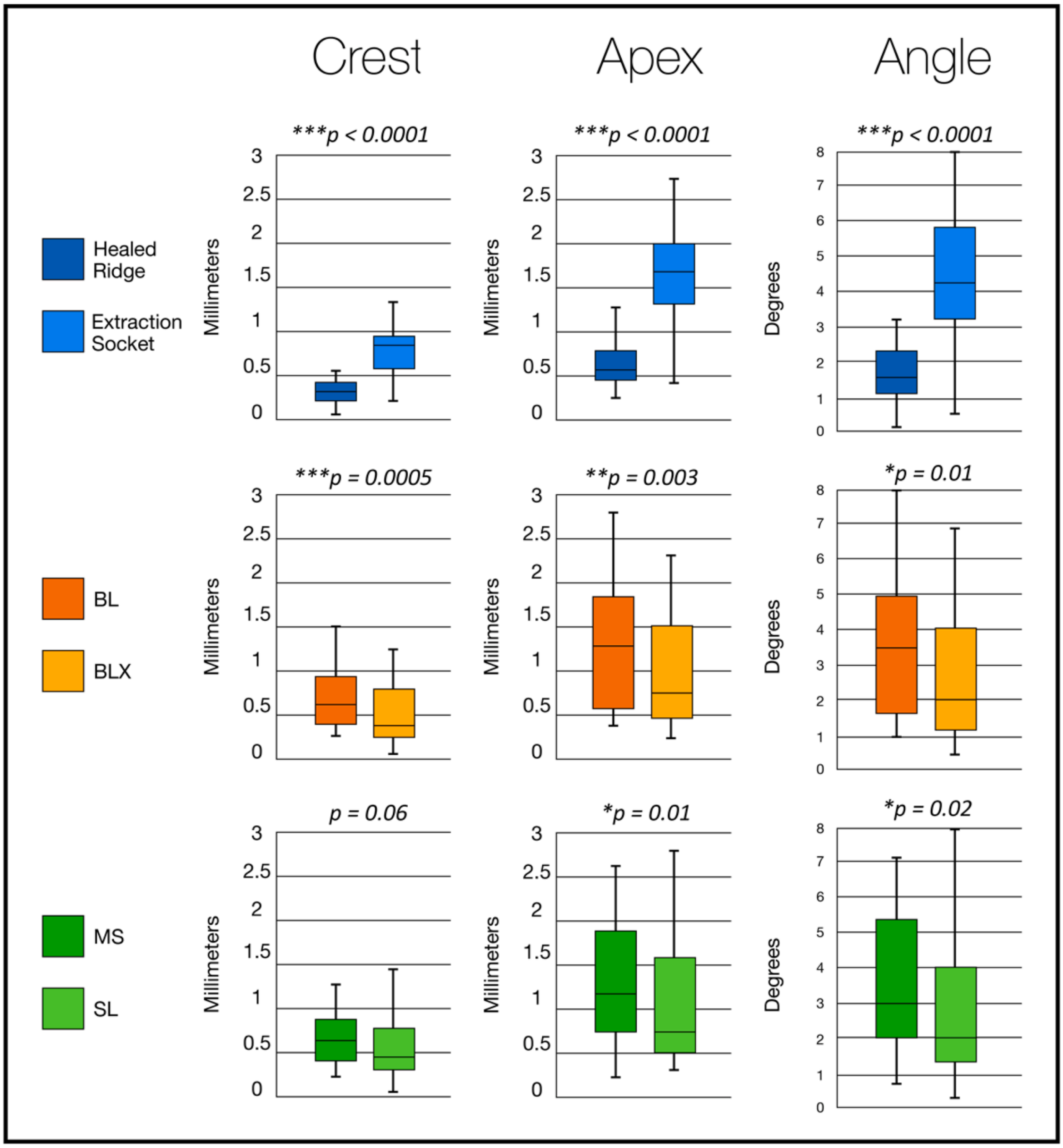

Fig. 3. Box plots demonstrating the effect of alveolar ridge morphology (blue colors), macroscopic design of the implant fixture (oranges colors), and guide-hole design (green colors), on the crestal, apical, and angular 3D implant deviations. (For interpretation of the references to colour in this figure legend, the reader is referred to the web version of this article.)

different manufacturers [25,26], accuracy may differ when using multiple sCAIS systems of one manufacturer. Findings pertaining to the influence of the macroscopic design of the implant fixture are in accordance with an *in vitro* study, where shallow-threaded tapered implants showed significantly less 3D deviation at the crest and apex levels than parallel-walled implants [13]. However, to the best of the authors' knowledge, this is the first study evaluating the accuracy of BLX implants with a deep-threaded tapered macro-design. Besides implant macro-design, a key factor influencing the accuracy of the final implant position might be found in system-dependent components, such as surgical drills or surgical keys. The BLX drills with a diameter of 2.2 mm, 2.8 mm, and 3.2 mm are two-edged twisted with a cutting-edge geometry reducing friction to the bony walls. Contrarily, only the initial BL drill (2.2 mm) is two-edged twisted whilst the larger diameter drills are three-edged twisted. Another possible hypothesis for the higher accuracy of BLX implants may be related to the differences of the implant connection geometries between the BLX (TorcFit) and BL (CrossFit) implants. Both TorcFit and CrossFit connection include a conical design, but only the TorcFit utilizes a flat top portion that provides a vertical stop for inserted components. However, the present study design is investigating both implant systems globally, and no conclusion on a single influencing factor should be drawn.

The design of the present study enabled the standardization of many variables that might affect clinical outcomes. However, there are several limitations, such as the effect of extended edentulous spaces/edentulism, other guide-hole designs (i.e., open, or closed sleeve), and macroscopic designs of the implant (i.e., different lengths, and diameters), that were not evaluated. These factors can also influence the accuracy of the final implant position, especially in socket morphologies where implant primary stability is required for treatment success. Furthermore, sample size calculation was carried out for each of the single factor's morphology of implant site, guide-hole design and implant macro-design, but not the investigated interaction terms, which may mask potential significance. Future *in vitro* and clinical studies are

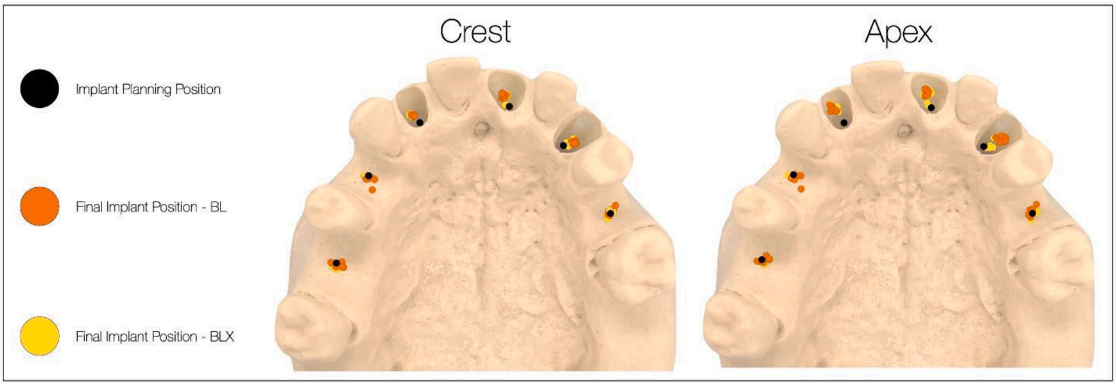

Fig. 4. Visual depiction of the deviations of the final implant position at the crestal and apical levels in BL (orange dots) and BLX implants (yellow dots) with respect to the preoperative implant planning position (black dots) at different alveolar ridge morphologies. BL: Parallel-walled with a shallow thread depth bone level implant; BLX: Tapered with a deep thread depth bone level implant. (For interpretation of the references to colour in this figure legend, the reader is referred to the web version of this article.)

needed to evaluate whether other alveolar ridge morphologies (i.e., fully edentulous ridge, longer-span partial edentulism, early soft tissue healing, partial bone healing), surgical variables (i.e., flap elevation, or flapless), implant macro-designs (i.e., implant body, length, diameter, thread design) and guide-hole designs (i.e., open, or closed sleeve) affect the accuracy and precision of implant placement via sCAIS.

5. Conclusions

Within the limitations of this *in vitro* study, the accuracy of the final implant position via sCAIS protocol is associated with the morphology of the alveolar ridge, guide-hole design, and macroscopic design of the implant. Implants placed in fresh extraction sockets have higher 3D deviations showing a facial drift of the final implant position compared to implants placed in a fully healed ridge. Surgical guides with sleeveless guide holes improve the accuracy of the final implant position as compared to the manufacturer's sleeve when design variables are under control. Deep-threaded tapered implants (BLX) had higher implant positional accuracy than shallow-threaded parallel-walled (BL) implants

Source of funding

This study was funded by the Fund for Dental Research of the Swiss Dental Association (Fund-Nr. 338-22).

Disclaimers

F.A.D has no conflicts of interest to report pertaining to the conduction of this study. E.C.Q has no conflicts of interest to report pertaining to the conduction of this study. V.C has no conflicts of interest to report pertaining to the conduction of this study. B.Y has no conflicts of interest to report pertaining to the conduction of this study. S.A.A received speaker and consultant honoraria from Straumann AG. C.R has no conflicts of interest to report pertaining to the conduction of this study.

CRediT authorship contribution statement

Fabrice Alain Dulla: Conceptualization, Methodology, Investigation, Formal analysis, Writing – original draft, Writing – review & editing. **Emilio Couso-Queiruga:** Visualization, Writing – review & editing. **Vivianne Chappuis:** Resources, Writing – review & editing. **Burak Yilmaz:** Writing – review & editing. **Samir Abou-Ayash:** Resources, Conceptualization, Methodology, Writing – review & editing. **Clemens Raabe:** Project administration, Funding acquisition, Conceptualization, Methodology, Investigation, Formal analysis, Writing – original draft, Writing – review & editing.

Declaration of Competing Interest

The authors declare that they have no known competing financial interests or personal relationships that could have appeared to influence the work reported in this paper.

The authors declare the following financial interests/personal relationships which may be considered as potential competing interests:

Samir Abou-Ayash: Speaker and consulting honoraria: Straumann AG

Acknowledgment

The authors would like to thank Dr. Lukas Martig for his efforts and support during the conduction of the study.

References

[1] P. Smitkarn, K. Subbalekha, N. Mattheos, A. Pimkhaokham, The accuracy of single-tooth implants placed using fully digital-guided surgery and freehand implant surgery, J. Clin. Periodontol. 46 (2019) 949–957, https://doi.org/10.1111/jcpe.13160.

[2] Z. Chen, J. Li, C.Y. Lin, H.L. Wang, Trend of scientific production on digital implant dentistry (1990-2019): a bibliometric study, Stomatol. Edu J. 7 (2020) 123–130, https://doi.org/10.25241/stomaeduj.2020.7(2).art.6.

[3] K.C. Oh, J.M. Park, J.S. Shim, J.H. Kim, J.E. Kim, J.H. Kim, Assessment of metal sleeve-free 3D-printed implant surgical guides, Dent. Mater. 35 (2019) 468–476, https://doi.org/10.1016/j.dental.2019.01.001.

[4] B. Vandenberghe, The digital patient - imaging science in dentistry, J. Dent. 74 (Suppl 1) (2018) S21–S26, https://doi.org/10.1016/J.JDENT.2018.04.019.

[5] F. Bover-Ramos, J. Viña-Almunia, J. Cervera-Ballester, M. Peñarrocha-Diago, B. García-Mira, Accuracy of implant placement with computer-guided surgery: a systematic review and meta-analysis comparing cadaver, clinical, and *in vitro* studies, Int. J. Oral Maxillofac. Implants 33 (2018) 101–115, https://doi.org/10.11607/jomi.5556.

[6] W. Zhou, Z. Liu, L. Song, C. ling Kuo, D.M. Shafer, Clinical factors affecting the accuracy of guided implant surgery- a systematic review and meta-analysis, J. Evid. Based Dent. Pract. 18 (2018) 28–40, https://doi.org/10.1016/J.JEBDP.2017.07.007.

[7] P. Henprasert, D.V. Dawson, T. El-Kerdani, X. Song, E. Couso-Queiruga, J. A. Holloway, Comparison of the accuracy of implant position using surgical guides fabricated by additive and subtractive techniques, J. Prosthodont. 29 (2020) 534–541, https://doi.org/10.1111/JOPR.13161.

[8] A. Tahmaseb, V. Wu, D. Wismeijer, W. Coucke, C. Evans, The accuracy of static computer-aided implant surgery: a systematic review and meta-analysis, Clin. Oral. Implants Res. 29 (2018) 416–435, https://doi.org/10.1111/clr.13346.

[9] J. Li, P.C. Meneghetti, M. Galli, G. Mendonca, Z. Chen, H. Wang, Open-sleeve templates for computer-assisted implant surgery at healed or extraction sockets: an *in vitro* comparison to closed-sleeve guided system and free-hand approach, Clin. Oral. Implants Res. 33 (2022) 757–767, https://doi.org/10.1111/clr.13957.

[10] M. Tattan, L. Chambrone, O. González-Martín, G. Avila-Ortiz, Static computer-aided, partially guided, and free-handed implant placement: a systematic review and meta-analysis of randomized controlled trials, Clin. Oral. Implants Res. 31 (2020) 889–916, https://doi.org/10.1111/CLR.13635.

[11] C.R. Adams, R. Ammoun, G.R. Deeb, S. Bencharit, Influence of metal guide sleeves on the accuracy and precision of dental implant placement using guided implant surgery: an *in vitro* study, J. Prosthodont. (2022), https://doi.org/10.1111/jopr.13503.

[12] K. El Kholy, R. Lazarin, S.F.M. Janner, K. Faerber, R. Buser, D. Buser, Influence of surgical guide support and implant site location on accuracy of static computer-assisted implant surgery, Clin. Oral. Implants Res. 30 (2019) 1067–1075, https://doi.org/10.1111/clr.13520.

[13] K. El Kholy, S. Ebenezer, J.G. Wittneben, R. Lazarin, D. Rousson, D. Buser, Influence of implant macrodesign and insertion connection technology on the accuracy of static computer-assisted implant surgery, Clin. Implant Dent. Relat. Res. 21 (2019) 1073–1079, https://doi.org/10.1111/cid.12836.

[14] Z. Chen, J. Li, P. Ceolin Meneghetti, M. Galli, G. Mendonça, H.L. Wang, Does guided level (fully or partially) influence implant placement accuracy at post-extraction sockets and healed sites? an *in vitro* study, Clin. Oral Investig. (2022), https://doi.org/10.1007/s00784-022-04512-y.

[15] M. Tallarico, M. Martinolli, Y.J. Kim, F. Cocchi, S.M. Meloni, A. Alushi, E. Xhanari, Accuracy of computer-assisted template-based implant placement using two different surgical templates designed with or without metallic sleeves: a randomized controlled trial, Dent. J. 7 (2019), https://doi.org/10.3390/dj7020041.

[16] S. Schnutenhaus, C. Edelmann, H. Rudolph, Does the macro design of an implant affect the accuracy of template-guided implantation? A prospective clinical study, Int. J. Implant. Dent. 7 (2021), https://doi.org/10.1186/s40729-021-00320-3.

[17] A. Pozzi, G. Polizzi, P.K. Moy, Guided surgery with tooth-supported templates for single missing teeth: a critical review, Eur. J. Oral Implantol. 9 (2016) 135–153.

[18] T. Joda, M. Ferrari, G.O. Gallucci, J.G. Wittneben, U. Brägger, Digital technology in fixed implant prosthodontics, Periodontol. 2000 73 (2017) 178–192, https://doi.org/10.1111/prd.12164.

[19] E. Couso-Queiruga, S. Stuhr, M. Tattan, L. Chambrone, G. Avila-Ortiz, Post-extraction dimensional changes: a systematic review and meta-analysis, J. Clin. Periodontol. 48 (2021) 126–144, https://doi.org/10.1111/jcpe.13390.

[20] E. Couso-Queiruga, H.A. Weber, C. Garaicoa-Pazmino, C. Barwacz, M. Kalleme, P. Galindo-Moreno, G. Avila-Ortiz, Influence of healing time on the outcomes of alveolar ridge preservation using a collagenated bovine bone xenograft: a randomized clinical trial, J. Clin. Periodontol. (2022), https://doi.org/10.1111/jcpe.13744.

[21] M.S. Tonetti, R.E. Jung, G. Avila-Ortiz, J. Blanco, J. Cosyn, S. Fickl, E. Figuero, M. Goldstein, F. Graziani, P. Madianos, A. Molina, J. Nart, G.E. Salvi, I. Sanz-Martin, D. Thoma, N. van Assche, F. Vignoletti, Management of the extraction socket and timing of implant placement: consensus report and clinical recommendations of group 3 of the XV european workshop in periodontology, J. Clin. Periodontol. 46 (Suppl 21) (2019) 183–194, https://doi.org/10.1111/JCPE.13131.

[22] C.H.F. Hämmerle, S.T. Chen, T.G. Wilson, Consensus statements and recommended clinical procedures regarding the placement of implants in extraction sockets, Int. J. Oral Maxillofac. Implants (19 Suppl) (2004) 26–28. https://pubmed.ncbi.nlm.nih.gov/15635943.

[23] D. Schneider, F. Schober, P. Grohmann, C.H.F. Hammerle, R.E. Jung, In-vitro evaluation of the tolerance of surgical instruments in templates for computer-assisted guided implantology produced by 3-D printing, Clin. Oral. Implants Res. 26 (2015) 320–325, https://doi.org/10.1111/clr.12327.

[24] Ł. Zadrożny, M. Czajkowska, M. Tallarico, L. Wagner, J. Markowski, E. Mijiritsky, M. Cicciù, Prosthetic surgical templates and dental implant site time preparation: an *in vitro* study, Prosthesis 4 (2022) 25–37, https://doi.org/10.3390/prosthesis4010004.

[25] V. Laederach, K. Mukaddam, M. Payer, A. Filippi, S. Kühl, Deviations of different systems for guided implant surgery, Clin. Oral. Implants Res. 28 (2017) 1147–1151, https://doi.org/10.1111/clr.12930.

[26] P. Sittikornpaiboon, S. Arunjaroensuk, B. Kaboosaya, K. Subbalekha, N. Mattheos, A. Pimkhaokham, Comparison of the accuracy of implant placement using different drilling systems for static computer-assisted implant surgery: a simulation-based experimental study, Clin. Implant Dent. Relat. Res. 23 (2021) 635–643, https://doi.org/10.1111/cid.13032.

[27] C.E. Misch, Chapter 11 - Bone Density: A Key Determinant for Treatment Planning. Dental Implant Prosthetics, 2nd ed, Mosby, 2015.

[28] J.J. Higgins, An Introduction to Modern Nonparametric Statistics, Brooks/Cole, 2004.

[29] R Core Team. R: A language and environment for statistical computing, R Foundation for Statistical Computing, Vienna, Austria, 2022. https://www.R-project.org/.

[30] M. Wang, X. Rausch-Fan, Y. Zhan, H. Shen, F. Liu, Comparison of implant placement accuracy in healed and fresh extraction sockets between static and dynamic computer-assisted implant surgery navigation systems: a model-based evaluation, Materials 15 (2022) 2806, https://doi.org/10.3390/ma15082806.

[31] M. Tallarico, M. Czajkowska, M. Cicciù, F. Giardina, A. Minciarelli, Ł. Zadrożny, C. J. Park, S.M. Meloni, Accuracy of surgical templates with and without metallic sleeves in case of partial arch restorations: a systematic review: accuracy of surgical templates with and without metallic sleeves, J. Dent. 115 (2021), https://doi.org/10.1016/j.jdent.2021.103852.

[32] K.C. Oh, J.S. Shim, J.M. Park, *In vitro* comparison between metal sleeve-free and metal sleeve-incorporated 3d-printed computer-assisted implant surgical guides, Materials 14 (2021) 1–10, https://doi.org/10.3390/ma14030615.

[33] M. Cassetta, A. di Mambro, G. di Giorgio, L.V. Stefanelli, E. Barbato, The influence of the tolerance between mechanical components on the accuracy of implants inserted with a stereolithographic surgical guide: a retrospective clinical study, Clin. Implant Dent. Relat. Res. 17 (2015) 580–588, https://doi.org/10.1111/cid.12120.

[34] A. Keßler, M. Dosch, M. Reymus, M. Folwaczny, Influence of 3D-printing method, resin material, and sterilization on the accuracy of virtually designed surgical implant guides, J. Prosthet. Dent. 128 (2022) 196–204, https://doi.org/10.1016/j.prosdent.2020.08.038.

[35] A. Unkovskiy, P.H.B. Bui, C. Schille, J. Geis-Gerstorfer, F. Huettig, S. Spintzyk, Objects build orientation, positioning, and curing influence dimensional accuracy and flexural properties of stereolithographically printed resin, Dent. Mater. 34 (2018) e324–e333, https://doi.org/10.1016/j.dental.2018.09.011.